INFECTION AND IMMUNITY, July 2010, p. 2956–2965 Vol. 78, No. 7
0019-9567/10/$12.00 doi:10.1128/IAI.01027-09

Dendritic Cells Inhibit the Progression of *Listeria monocytogenes* Intracellular Infection by Retaining Bacteria in Major Histocompatibility Complex Class II-Rich Phagosomes and by Limiting Cytosolic Growth▽†

Marlena M. Westcott, Curtis J. Henry,‡ Jacqueline E. Amis, and Elizabeth M. Hiltbold*

Department of Microbiology and Immunology, Wake Forest University School of Medicine, Winston-Salem, North Carolina 27157[1]

Received 8 September 2009/Returned for modification 16 December 2009/Accepted 12 April 2010

Dendritic cells (DC) provide a suboptimal niche for the growth of *Listeria monocytogenes*, a facultative intracellular bacterial pathogen of immunocompromised and pregnant hosts. This is due in part to a failure of large numbers of bacteria to escape to the cytosol, an essential step in the intracellular life cycle that is mediated by listeriolysin O (LLO). Here, we demonstrate that wild-type bacteria that failed to enter the cytosol of bone marrow-derived DC were retained in a LAMP2$^+$ compartment. An isogenic *L. monocytogenes* strain that produces an LLO protein with reduced pore-forming activity had a severe escape and growth phenotype in DC. Few mutant bacteria entered the cytosol in the first 2 h and were instead found in LAMP2$^+$, major histocompatibility complex class II$^+$ (MHC-II$^+$) H2-DM vesicles characteristic of MHC-II antigen loading compartments (MIIC). In contrast, the mutant had a minor phenotype in bone marrow-derived macrophages (BMM) despite the reduced LLO activity. In the first hour, DC phagosomes acidified to a pH that was, on average, half a point higher than that of BMM phagosomes. Unlike BMM, *L. monocytogenes* growth in DC was minimal after 5 h, and consequently, DC remained viable and matured late in infection. Taken together, the data are consistent with a model in which phagosomal maturation events associated with the acquisition of MHC-II molecules present a suboptimal environment for *L. monocytogenes* escape to the DC cytosol, possibly by limiting the activity of LLO. This, in combination with an undefined mechanism that controls bacterial growth late in infection, promotes DC survival during the critical maturation response.

Dendritic cells (DC) comprise a heterogeneous group of antigen-presenting cells (APC) that have the unique capacity to activate naïve T cells, and thus they are required for the initiation of an adaptive immune response (4). Immature DC link the innate to the adaptive immune response by sampling material from the local environment and differentiating in a manner appropriate to the ingested cargo. Maturation into APC capable of presenting antigens for the initiation of an adaptive immune response results when DC pattern recognition receptors encounter molecular signatures associated with pathogens (4, 25). In recent years, studies using predominantly bone marrow-derived myeloid DC and model antigens have indicated that the unique ability of DC to induce primary T-cell responses is a function of endosomal/lysosomal specializations that effectively preserve immunogenic peptides (26, 34, 43). Unlike other professional APC, antigen processing and presentation in DC is coupled to the receipt of appropriate maturation signals (25, 26). Immature DC have a high capacity to ingest soluble and particulate material and sequester it in major histocompatibility complex class II (MHC-II)-rich compartments (MIIC) (19, 30). The degradation and loading of peptides onto MHC-II, as well as the delivery to and retention of peptide-MHC complexes on the cell surface, is enhanced after the receipt and assimilation of inflammatory signals (11, 19, 30, 44). Recent evidence suggests that antigen degradation is limited in immature DC endosomes and lysosomes relative to that of macrophages by lower protease content as well as by an acidification response that controls the rate and extent of proteolysis (14, 26, 42). These adaptations have been proposed to prevent the destruction of immunogenic epitopes destined for presentation to T cells (14, 26, 35).

Listeria monocytogenes belongs to a class of intracellular pathogens that must escape the host cell endosomal/lysosomal system in order to grow. *L. monocytogenes* infects a broad range of cell types, including DC, and the intracellular life cycle has been characterized in detail (31). The growth stage of the *L. monocytogenes* life cycle proceeds after the rupture of the phagosomal membrane by a pH- and cholesterol-dependent pore-forming cytolysin, listeriolysin O (LLO), with the assistance of a bacterial phosphatidylinositol-specific phospholipase C (PI-PLC). Within 30 min of uptake by macrophages, *L. monocytogenes* escapes from LAMP1-negative, late endosomal vesicles, which acidify to pH 5.5, providing an optimal environment for LLO-mediated pore formation (5, 18, 28). Consequently, the majority of *L. monocytogenes* can be found free and replicating in the macrophage cytosol in the first hour of infection. Bacterial escape is inefficient after phagosomal fusion with lysosomes (18), presumably due to a harsh envi-

* Corresponding author. Mailing address: Department of Microbiology and Immunology, Wake Forest University School of Medicine, Medical Center Blvd., Winston-Salem, NC 27157. Phone: (336) 716-8246. Fax: (336) 716-9928. E-mail: bhiltbol@wfubmc.edu.

† Supplemental material for this article may be found at http://iai.asm.org/.

‡ Present address: Department of Biochemistry and Molecular Genetics, University of Colorado at Denver; 12801 East 17th Ave., Aurora, CO 80045.

▽ Published ahead of print on 19 April 2010.

ronment (low pH, high proteolysis) that does not support LLO activity. *L. monocytogenes* thus takes advantage of a small window of opportunity within minutes after ingestion by macrophages, during which the phagosomal conditions are favorable for LLO to mediate bacterial escape to the cytosol. Once in the cytosol, *L. monocytogenes* recruits the host cell actin machinery to spread to adjacent cells by a process of intercellular spread. Escape from secondary spreading vacuoles, mediated by LLO in combination with two bacterial phospholipases (PI-PLC and a broad-range PLC, PC-PLC) (1), allows the infection to progress while shielding the bacteria from extracellular immune defenses of the host. The intracellular lifestyle dictates that clearance of the pathogen requires the processing and presentation of bacterial antigens via the MHC-I pathway and the activation of a $CD8^+$ T-cell response (22). The presentation of antigens via the MHC-II pathway and activation of a $CD4^+$ T-cell response is necessary for the maintenance of long-term $CD8^+$ T-cell memory (41).

DC mature in response to infection with wild-type (WT) *L. monocytogenes* (3, 9, 27) and are required for the initiation of an adaptive immune response in the murine intravenous model (21). We have previously reported that bone marrow-derived DC have the capacity to restrict large numbers of *L. monocytogenes* to a membrane-bound compartment and, consequently, to limit their intracellular growth (50). This is in contrast to bone marrow-derived macrophages (BMM), which support relatively unrestricted bacterial growth in the cytosol. Consistent with these findings, DC become infected with *L. monocytogenes in vivo*, but unlike macrophages, they do not appear to provide a significant niche for bacterial replication (2, 27). Given the critical role of DC in the immune response, the limitation of intracellular bacterial infection may preserve and enhance their specialized antigen-presenting function. Therefore, to begin to address how DC control *L. monocytogenes* growth, we examined the characteristics of DC phagosomes early after infection. Evidence is provided that phagosomal maturation events associated with the acquisition of MHC-II molecules reduce the efficiency of *L. monocytogenes* escape to the DC cytosol, possibly by presenting suboptimal environmental conditions for LLO. Along with an additional as-yet undefined mechanism that controls the extent of bacterial growth in the cytosol, these DC-specific responses to *L. monocytogenes* infection preserve cellular integrity during the course of the maturation response.

MATERIALS AND METHODS

Antibodies and reagents. Primary antibodies were used at a final concentration of 5 μg/ml. Rat anti-mouse (ms) LAMP2 and rat anti-ms H2-DM were from eBioscience (SanDiego, CA), and anti-ms Ia^b (clone AF6) and rat anti-ms CD86 were from BD Biosciences (San Jose, CA). Rabbit polyclonal anti-*Listeria* antibody (5346858; Difco) was used at a 1:300 dilution. The following reagents were from Invitrogen/Molecular Probes (Carlsbad, CA): Alexa Fluor-conjugated secondary antibodies AF488-goat anti-rat IgG, AF546-goat anti-ms IgG, AF488, AF568, or Cy5-labeled goat-anti-rabbit IgG (1:500); Alexa Fluor-conjugated phalloidin (1:50), lysotracker red (LTR); carboxyfluorescein succinimidyl ester (CFSE); and AF647 succinimidyl ester (AF647SE). CFSE and AF647SE were prepared as 5-mg/ml stocks in dimethylsulfoxide (DMSO) and stored at −20°C. Bafilomycin A_1 ($BafA_1$) monensin, and nigericin were from Sigma (St. Louis, MO).

Bacteria. The WT strain of *L. monocytogenes* used in these studies was 10403S. The isogenic strain, DP-L4044, carrying an LLO point mutation (G486D) was obtained from Daniel Portnoy and has been described previously (13). For infection, bacteria were grown for 16 to 18 h in static brain heart infusion (BHI) broth cultures at 30°C.

Cells. DC and BMM were derived from C57BL/6 bone marrow (isolated from female, 10- to 24-week-old mice) as described previously (50). Briefly, bone marrow devoid of red blood cells was cultured with 10 ng/ml granulocyte-macrophage colony-stimulating factor (GM-CSF) for 6 days, and DC were purified by CD11c-positive selection using magnetic beads (Miltenyi, Auburn, CA). $CD11c^+$ cells (>95% purity) were recultured overnight (with GM-CSF) and infected on day 7. BMM were harvested after 6 days of culture with 10% supernatant from CSF-1-transfected NIH-3T3 cells. As for DC, cells were recultured overnight (with CSF-1) and infected on day 7.

Infections. The intracellular growth assay was performed as described previously (50). Briefly, cell monolayers grown on 12-mm glass coverslips were infected with *L. monocytogenes* (multiplicity of infection [MOI], 0.30) for 1 h, washed three times, and treated with 10 μg/ml gentamicin to kill extracellular bacteria. Cell lysates were prepared at the indicated time points, and dilutions were plated on LB agar to enumerate CFU. For confocal microscopy and pH studies, an MOI of 3.0 to 10.0 was used, and changes to the basic infection protocol are indicated in the corresponding sections of Materials and Methods and in the figure legends.

Evaluation of *L. monocytogenes* escape to the cytosol. Infected cells were fixed, permeabilized, and stained for total bacteria (using anti-*Listeria* antibody followed by AF568-labeled goat anti-rabbit IgG) and actin (using AF488-labeled phalloidin). Individual bacteria were scored as cytosolic ($phalloidin^+$) or noncytosolic ($phalloidin^-$) by epifluorescence microscopy using a Nikon Eclipse TE300 microscope equipped with a 100× oil immersion lens.

Laser-scanning confocal microscopy. Cells were infected on glass coverslips as described in the figure legends, fixed, permeabilized, and stained for total *L. monocytogenes* in combination with LAMP2, MHC-II (Ia^b), or H2-DM. For qualitative pH analysis, DC were pulsed for the final 30 min of infection with 1 μM LTR and washed extensively prior to fixation and analysis. Cells were analyzed for the colocalization of bacteria with markers using a Zeiss Axiovert 100 M laser-scanning confocal microscope and Zeiss LSM image analysis software. Serial 0.5- to 1.0-μm optical sections through multiple fields of infected cells were analyzed. The number of bacteria scored for colocalization with individual markers is indicated in the figures and/or legends.

Labeling of *L. monocytogenes* with CFSE and AF647. *L. monocytogenes* LLO G486D was either single labeled with CFSE or dual labeled with CFSE and AF647SE for pH experiments. Washed, stationary-phase bacteria (2×10^8) were resuspended in 0.5 ml PBS, pH 8.3, containing CFSE (100 μM). The labeling reaction was performed for 10 min at 37°C with end-over-end rotation and stopped by adding 0.5 ml fetal calf serum (FCS). Bacteria were washed twice with PBS (pH 7.2) containing 3% FCS and once with PBS (pH 7.2). CFSE-labeled bacteria were resuspended in 0.5 ml PBS, pH 8.3, containing AF647 succinimidyl ester (100 μM). The labeling reaction mixture and washes were the same as those described for the CFSE protocol. Bacterial viability was minimally affected by the labeling reactions (>80% viable).

Infection for quantitative phagosomal pH assay. The phagosomal pH assay was adapted for use with live bacteria from published assays (35, 46). DC and BMM monolayers grown in 12-well dishes were infected in a volume of 0.5 ml with dual-labeled *L. monocytogenes* (MOI, 10) for 10 min at 37°C, 5% CO_2, washed three times, and chased with fresh medium for 35 min. Cells were harvested following a 5-min treatment with Accutase nonenzymatic cell detachment solution (ISC BioExpress, Kaysville, UT) and resuspended in media of defined pH (Invitrogen CO_2-independent medium, adjusted to pH 4.5 to 7.5 in 0.5-ml steps) containing the K^+ and Na^+ ionophores nigericin (20 μM) and monensin (4 μM) to equilibrate the intracellular and extracellular pH. Identical samples were incubated in medium adjusted to the same pH but without ionophores. CFSE (pH-sensitive) and AF647 (pH-insensitive) fluorescence for both sets of samples were measured by flow cytometry with gating on the predominant infected cell population (excluding outliers). A standard curve was generated by plotting the ratio of the geometric mean fluorescence intensity (MFI) of CFSE to AF647. The expression of the data as a ratio of pH-sensitive to pH-insensitive fluorescence controls for potential differences in bacterial uptake by the two cell types. The intracellular pH was defined using GraphPad Prism software by the point of intersection of the two curves (i.e., those with and without ionophores).

Cell viability assay. The viability of DC and BMM monolayers after infection with *L. monocytogenes* as described for intracellular growth assays was evaluated by collecting supernatants at time points over the course of 12 h and measuring lactate dehydrogenase (LDH) levels by using the Promega Cytotox 96 assay kit according to the manufacturer's instructions.

Evaluation of DC maturation. CD11c-purified DC were infected for 1 h with WT *L. monocytogenes* (MOI, 0.30) in 12-well dishes. At 1 h, cells were washed

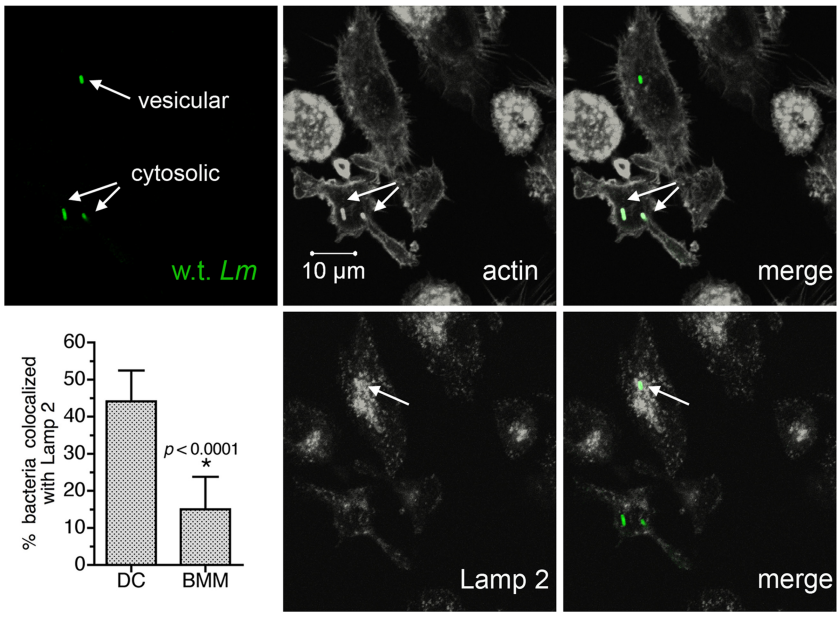

FIG. 1. DC retain significant numbers of *L. monocytogenes* cells in a LAMP2$^+$ compartment. DC were infected for 30 min with wild-type *L. monocytogenes* 10403S, washed, and chased for 1 to 2.5 h. Cells were fixed and permeabilized, and three-color staining for total bacteria, LAMP2, and actin was performed. The three-color confocal images, depicting a 0.5-μm optical section through a representative field of DC infected for 3 h, were split, and the LAMP2 and actin images were converted to grayscale. LAMP2 and actin images overlaid with bacteria (green) are also shown. Cumulative results indicating the percentage of bacteria colocalized with LAMP2 (mean ± standard deviation) from seven (DC) and six experiments (BMM) are shown. Significance was determined by unpaired Student's *t* test.

and 10 μg/ml gentamicin was added. At 1.5 and 24 h after infection, cells were harvested using Accutase per the pH assay. For the quantitative analysis of maturation, cells were stained with APC-conjugated hamster anti-mouse CD11c and phycoerythrin (PE)-conjugated rat anti-mouse CD86 (BD Pharmingen) and analyzed by flow cytometry (FACSCalibur; Becton Dickinson) with gating on CD11c$^+$ cells (>90% of the population). Additional samples of infected cells grown on glass coverslips were fixed and stained for immunofluorescence microscopy at the same time points using anti-CD86 and anti-*Listeria* antibodies as described previously (50).

Statistical analysis. Significance, where indicated, was determined by the two-tailed unpaired Student's *t* test.

RESULTS

Wild-type *L. monocytogenes* is targeted to a LAMP2$^+$ compartment in the first hours after DC infection. To determine how DC inhibit *L. monocytogenes* egress to the cytosol, we characterized *L. monocytogenes*-containing phagosomes early after infection. Cells initially were evaluated between 1.5 and 3 h after infection, a time frame during which many bacteria remained trapped in DC but were free in the BMM cytosol (50). We first addressed the stage of phagosomal maturation at that time by assessing intracellular bacteria for colocalization with the endosomal/lysosomal marker LAMP2. Both cytosolic and noncytosolic bacteria were found in DC, which is consistent with our previous results (50). Bacteria that were not actin$^+$ (cytosolic) colocalized with the LAMP2 marker (Fig. 1). Cumulative results from multiple experiments demonstrated that in DC, roughly half of all intracellular bacteria were localized to LAMP2$^+$ vesicles between 1.5 and 3 h of infection. Consistent with rapid bacterial escape to the cytosol, a significantly smaller percentage of bacteria were found in LAMP2$^+$ vesicles in BMM (approximately 15%, compared to 45% in DC). As we reported previously (50), subpopulations of DC appeared to preferentially trap bacteria or support escape to the cytosol; 53% ± 7% of infected DC contained exclusively LAMP2$^+$ bacteria, 27% ± 2% contained exclusively actin$^+$ bacteria, and the remainder showed a mixed phenotype ($n = 3$ experiments). In contrast to the results with LAMP2, bacteria did not colocalize with Rab5a, an early endosomal marker, during the same time frame of DC infection (data not shown). Therefore, wild-type *L. monocytogenes* organisms that failed to escape to the cytosol were trapped in a late endosomal or lysosomal compartment in the first hours after DC infection.

An LLO activity mutant has a severe escape and growth defect in DC. To explain the DC-specific escape and growth phenotype, we hypothesized that LLO function is compromised in the DC phagosomal environment. Initially we determined that as is the case for macrophages (20), an LLO deletion mutant (DP-L2161) did not escape from phagosomes or grow in DC, demonstrating a requirement for LLO in this cell type (data not shown). Consistent with the hypothesis that LLO function is compromised in DC, we observed differential behavior in DC and BMM of an isogenic *L. monocytogenes* strain, DP-L4044, that carries a point mutation in LLO. The G486D substitution, which resides in the carboxy-terminal membrane-binding domain of LLO, confers a 100-fold reduction in toxin activity (13). Despite producing an LLO protein with reduced membrane lytic activity, the mutant has a relatively minor phenotype in macrophages (13). As we reported previously (50), DC supported a 1-log increase in intracellular CFU when infected with the WT strain (Fig. 2a, open squares) compared to an approximately 2-log increase in BMM (open circles). The growth defect in DC was a function of both a slower initial bacterial doubling time, as we reported previ-

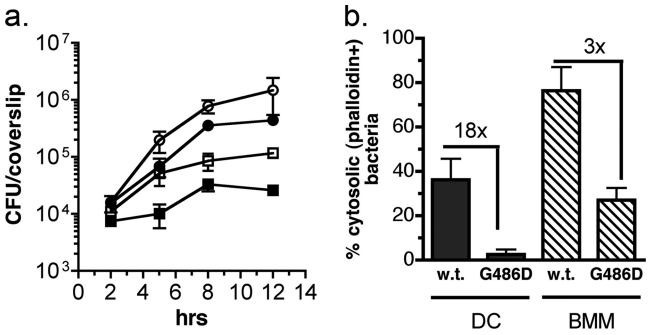

FIG. 2. Differential growth of wild-type (10403S) and LLO G486D mutants in DC and BMM. (a) DC and BMM were infected with 10403S (open symbols) or the LLO G486D mutant (closed symbols), and intracellular growth was measured for 12 h as described in Materials and Methods. Cumulative results from multiple experiments are shown; points represent the means ± standard deviations from 9 to 12 coverslips per time point for DC (squares) and 6 to 9 coverslips per time point for BMM (circles). To normalize for the number of CFU at 2 h, the G486D mutant was added at a 3-fold-higher MOI than that for wild-type bacteria for both DC and BMM. (b) Additional coverslips were processed for fluorescence microscopy at 1.5 to 3.0 h postinfection, and individual bacteria were scored as cytosolic or noncytosolic based on staining for total bacteria and for actin. The percentage of cytosolic bacteria (phalloidin$^+$ bacteria/total bacteria) and the fold decrease for the mutant compared to the level for the WT is shown for each cell type. The results are from three (BMM) or seven (DC) independent experiments. The total numbers of bacteria analyzed were the following: for DC, $n = 640$ (WT) and 741 (G486D); for BMM, $n = 1{,}109$ (WT) and 551 (G486D).

ously (50), and a failure of *L. monocytogenes* to replicate to a significant extent after 5 h. Notably, the LLO G486D mutant had a more dramatic growth defect in DC than did WT bacteria; the number of intracellular mutant bacteria increased only 3-fold during 12 h (closed squares). A long lag period between 2 and 5 h for the mutant strain reflected few bacteria in the cytosol, which was quantitated at 2.5 h by staining infected cells for actin-associated bacteria (Fig. 2b). Specifically, the percentage of bacteria in the cytosol was 18-fold lower for the LLO G486D mutant than for wild-type bacteria in DC. Regardless of infection dose (strength of microbial signal), the LLO G486D mutant was severely defective in its ability to enter the DC cytosol. At multiplicities of infection of 5.0, 1.0, and 0.2, the level of bacteria in the cytosol at 3 h was 8 ($n = 246$), 13 ($n = 117$), and 3% ($n = 87$), respectively. Further, after a small burst of replication between 5 and 8 h, the LLO G486D mutant stopped growing, as observed for WT bacteria. In contrast, the LLO G486D mutant had a mild phenotype relative to that of wild-type bacteria in BMM as reported previously (13). The percentage of bacteria in the cytosol was only 3-fold reduced for LLO G486D compared to the level for the WT in BMM, and this translated to a modest reduction in growth. Although gentamicin enters DC more effectively than it enters BMM (M. M. Westcott and E. M. Hiltbold, unpublished data), we determined that the bacterial phenotypes in DC were not due solely to gentamicin entering the intracellular DC compartment, as similar results were obtained when the drug was reduced in concentration, removed at 2 h, or eliminated completely (in conjunction with extensive washing; data not shown).

Therefore, when LLO activity was limiting, the escape and growth defect in DC was significantly amplified, while even low levels of active LLO were sufficient for bacterial escape to the BMM cytosol. Since the WT and mutant *L. monocytogenes* strains differed only in the LLO G486D substitution, the data are consistent with a more restrictive environment for LLO in DC phagosomes. Further, the cessation of bacterial growth after 5 h indicates an additional level of DC-mediated control over bacteria that had successfully entered the cytosol.

Live bacteria are targeted in the first hour to MHC-II-rich vesicles. The presence of LAMP2 is indicative of a compartment that has matured to a late endosomal or lysosomal stage (15). To define the characteristics of the *L. monocytogenes*-containing DC compartment further, we utilized the LLO G486D mutant, in which >97% of bacteria failed to enter the cytosol in the first 2 h after infection (Fig. 2b), allowing an almost exclusive focus on phagosomal bacteria for the analysis. A hallmark phenotype of immature DC is the colocalization of MHC-II with the MHC-II-like chaperone, H2-DM, in late endosomal and lysosomal vesicles (MIIC), while mature DC export MHC-II molecules to the cell surface, retaining vesicular H2-DM. The two patterns are clearly distinguishable by immunofluorescence staining (30). DC used in the current studies had the pattern characteristic of immature cells (Fig. 3a) prior to infection with *L. monocytogenes* (for comparison, the mature DC staining pattern also is shown). To determine if the LAMP2$^+$ vesicles identified in the previous experiments were MIIC, infected DC were stained for H2-DM or LAMP2 (green) and total *L. monocytogenes* (red). As shown in Fig. 3b, >90% of LLO G486D mutant bacteria colocalized with H2-DM (top, three-dimensional reconstructed image; bottom, optical sections through the same cell) and LAMP2 (graph in Fig. 3b; photomicrographs are not shown). Similar results were obtained with wild-type bacteria analyzed at 3 h (Fig. 3c), except that fewer colocalized with H2-DM because they had entered the cytosol (59% colocalized with H2-DM, and 41% were in the cytosol; $n = 81$). Also illustrated in Fig. 3c, vesicles retaining wild-type bacteria contained both H2-DM (green) and MHC-II (red). Therefore, *L. monocytogenes* cells that failed to escape to the DC cytosol by 1 h were contained within vesicles with characteristics of MIIC.

Early *L. monocytogenes*-containing DC vesicles acidify. The differential behavior of the LLO activity mutant G486D in DC compared to that in BMM raised the possibility that the defect in bacterial escape from DC phagosomes was a function of a more restrictive environment for LLO. LLO-mediated pore formation is a pH-dependent process, proceeding most effectively at pH 5.5 (16, 32). Recent reports have indicated that DC phagosomes have the capacity to remain pH neutral for several hours after the ingestion of cargo, an adaptation that prevents the premature destruction of antigenic epitopes (35). We therefore hypothesized that the enhanced retention of *L. monocytogenes* in DC phagosomes was due to an insufficient acidification response. We utilized several approaches to determine if early *L. monocytogenes*-containing DC phagosomes acidify. First, we took advantage of the pH sensitivity of the fluorescein derivative, CFSE. Specifically, CFSE fluorescence decreases with decreasing pH, and the labeling of phagocytic cargo with CFSE (and other fluorescein derivatives) has been used as a tool to monitor changes in intracellular pH (36).

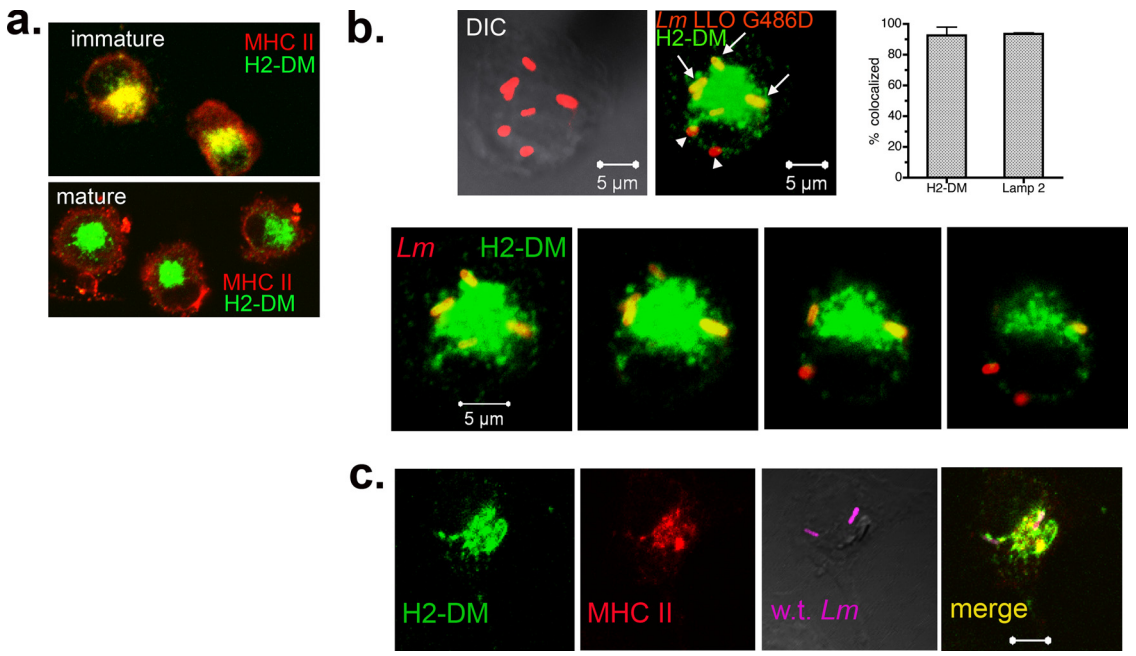

FIG. 3. *L. monocytogenes* is retained in an MHC-II-rich DC compartment. (a) Uninfected DC were fixed, permeabilized, and stained for MHC-II (red) and the MHC-II accessory molecule H2-DM (green). Two distinct staining patterns are shown, that of immature DC (day 7 adherent cells) and that of mature DC (day 7 nonadherent cells immobilized on poly-L-lysine-coated coverslips). In the former, which is representative of DC used in the current studies, MHC-II and H2-DM colocalize in intracellular vesicles. (b) DC were infected with the LLO G486D strain for a total of 1 to 3 h. Cells were stained for total *L. monocytogenes* and H2-DM and scored for the colocalization of bacteria with H2-DM by confocal microscopy. The top panel shows a representative z-stacked image (1-μm optical sections, 8 μm thick) with bacteria colocalized (arrows) and not colocalized (arrow heads) with H2-DM. The bottom panel depicts four optical sections through the same cell. The percentage of bacteria colocalized with H2-DM (n = 277; three independent experiments) and LAMP2 (n = 177; two independent experiments) is shown in the graph. DIC, differential interference contrast. (c) Optical section (0.5 μm) through a DC infected with WT *L. monocytogenes* for 3 h. The first two panels show the colocalization of H2-DM (green) with MHC-II (red) in intracellular vesicles, and the second two panels show the colocalization of *L. monocytogenes* (magenta) with both markers (yellow).

First, DC were infected with live CFSE-labeled LLO G486D for 1 h in the presence or absence of $BafA_1$. $BafA_1$ blocks phagosomal acidification by inhibiting the ATP-dependent vacuolar proton pump (vATPase) (8) and has been shown to inhibit the escape of *L. monocytogenes* to the macrophage cytosol (5, 28). We reasoned that if DC phagosomes remained in the pH-neutral range early after the ingestion of *L. monocytogenes*, then the fluorescence intensity of CFSE-labeled phagosomal *L. monocytogenes* would be similar in the presence and absence of $BafA_1$. As shown in Fig. 4a, the CFSE-positive population (representing infected DC) had a 3-fold greater mean fluorescence intensity (MFI) in the presence of $BafA_1$ (dotted histogram) than in the absence of $BafA_1$ (solid histogram), suggesting that DC phagosomes did in fact acidify in the first hour after infection.

These results were confirmed by labeling infected cells with lysotracker red (LTR), a membrane-permeable fluorescent dye that accumulates in acidic vesicles (47). DC were infected for 30 min, washed, chased for 30 min in the presence of LTR, and examined by confocal microscopy. As shown in Fig. 4b, LTR signals that ranged in intensity from negative/weak to bright were observed, with 84% of bacteria localizing to LTR-positive vesicles at 1 h. Taken together with the flow cytometry data presented in Fig. 4a, the results indicate that *L. monocytogenes*-containing DC phagosomes acidified in the first hour after infection.

***L. monocytogenes*-containing DC phagosomes have a modestly elevated pH relative to that of BMM phagosomes.** The qualitative analyses described above indicated that *L. monocytogenes*-containing DC phagosomes acidified to some extent during the course of 1 h. However, the possibility remained that the acidification response was insufficient for optimal LLO-mediated pore formation. We therefore modified published flow cytometry-based assays (35, 46) to measure the pH of DC phagosomes containing live *L. monocytogenes* early after infection. Several factors were considered in the experimental design. First, *L. monocytogenes* LLO G486D was used to minimize bacterial entry into the cytosol. Second, the pulse/chase infection protocol was designed to allow the earliest pH measurement at a point at which the majority of bacteria were intracellular and still in vesicles in both DC and BMM (approximately 45 min total infection time). Cells were infected with live bacteria that were dual labeled with CFSE (pH sensitive) and AF647 (pH insensitive), and the pH of *L. monocytogenes*-containing phagosomes was measured by gating on cells that were $CFSE^+$ and $AF647^+$ (see Fig. S1 in the supplemental material). As described in Materials and Methods, the data are reported as a ratio of pH-sensitive (CFSE) to pH-insensitive (AF647) fluorescence, which controls for potential differences in the uptake of the cargo by the two cell types. A representative experiment is illustrated in Fig. 5a, in which the DC phagosomal pH was determined to be 5.9. Re-

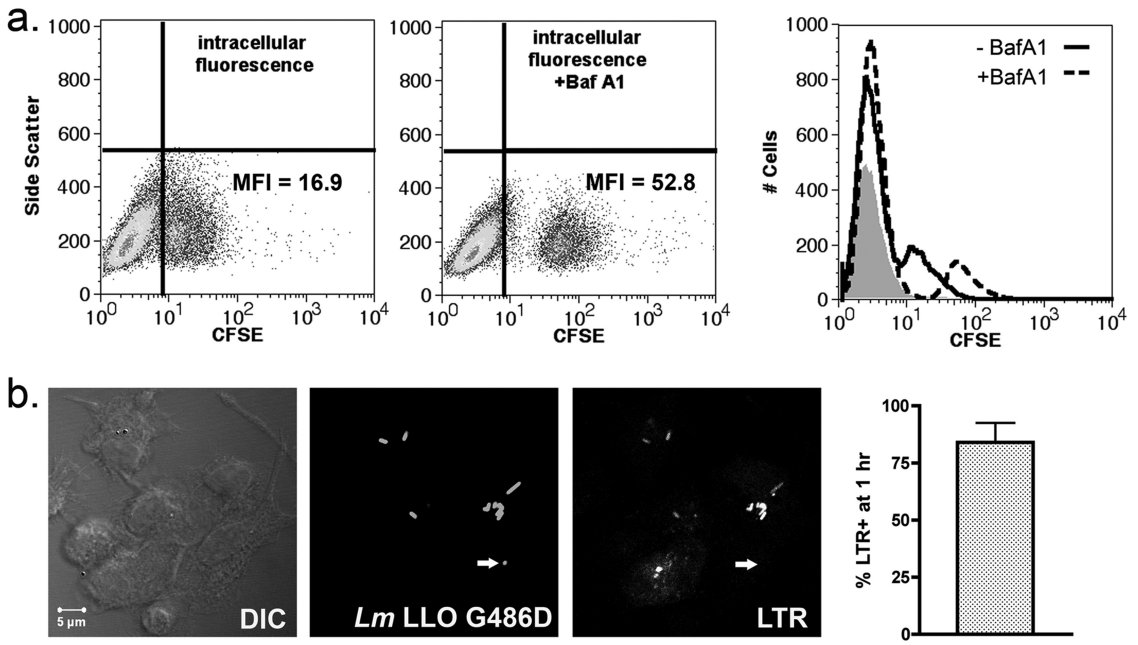

FIG. 4. *L. monocytogenes*-containing DC compartment acidifies by 1 h. (a) DC were pretreated for 30 min with $BafA_1$ (0.5 μM), infected for 30 min with CFSE-labeled LLO G486D, washed, and chased in the presence of $BafA_1$ for an additional 30 min. Intracellular CFSE fluorescence in the presence and absence of $BafA_1$ was measured by flow cytometry. The MFI of the $CFSE^+$ gate is shown. Histograms represent fluorescence intensity in the absence (solid line) and presence (dotted line) of $BafA_1$. The shaded histogram represents cells infected with unlabeled bacteria. Data represent one of three experiments with similar results. (b) DC were infected with unlabeled LLO G486D as described above and chased in the presence of LTR (1 μM) (red). Cells were fixed, permeabilized, and stained for total *L. monocytogenes* using an Alexfluor 488-conjugated secondary antibody (green). Bacteria that colocalized with LTR were scored by confocal microscopy. The single-channel images (converted to grayscale) depict a 0.5-μm optical section through a representative field. The arrow indicates the one bacterium in the field that does not colocalize with LTR. A total of 259 bacteria were scored in three independent experiments (n = 84, 114, and 61), and the results are expressed as percent bacteria localized to LTR^+ vesicles (% LTR^+).

sults from multiple independent determinations, shown in Fig. 5b, indicate a modest but significant difference in the acidification response of the two cell types. While the population of DC phagosomes was approaching or had reached the optimal pH for LLO pore-forming activity (pH as high as 6.0 with a mean of 5.5), BMM phagosomes had reached or surpassed it in the same time frame (pH as low as 4.5 with a mean of 5.0). These results provide further evidence that *L. monocytogenes*-containing DC phagosomes do in fact acidify, but they imply that the rate or extent of acidification is different for the two cell types. Nevertheless, within the 1-h time frame examined, DC phagosomes, like BMM phagosomes, reached a pH that was within the effective range for LLO (pH 5.0 to 6.0).

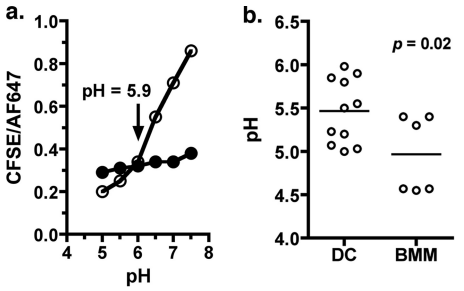

FIG. 5. Quantitative analysis of DC phagosomal pH in the first hour of infection. (a) DC were infected with dual-labeled LLO G486D (MOI, 10) for 10 min, washed, and chased for 35 min (total infection time, 45 min). Cells were harvested and exposed to media of defined pH in the presence (open circles) or absence (closed circles) of ionophores as described in Materials and Methods. CFSE and AF647 intracellular fluorescence were measured by flow cytometry after gating on the predominant infected cell population. The ratio of CFSE/AF647 mean fluorescence intensity (MFI) was plotted as a function of pH. (b) Cumulative results for DC (10 independent determinations) and BMM (infected as per DC; 6 independent determinations). The line denotes the mean pH for each group of experiments. Significance was determined by unpaired Student's t test.

Control of intracellular *L. monocytogenes* infection promotes DC survival. During the course of intracellular growth experiments, we observed that while BMM showed signs of cytotoxicity at late stages of infection (8 to 24 h), coincident with high numbers of bacteria replicating in the cytosol, cytotoxicity was less apparent in infected DC. To evaluate this observation quantitatively, we assessed cellular viability by measuring LDH release from cells infected with wild-type *L. monocytogenes* during the course of 12 h. The growth curve performed in parallel with LDH measurement is one of the multiple experiments depicted in Fig. 2a. Limited bacterial replication in DC preserved cellular viability as shown in Fig. 6a, while unrestricted bacterial growth in BMM led to decreased cellular viability starting at about 8 h (Fig. 6a). Consistent with these findings, the examination of DC and BMM monolayers at 24 h after infection by differential staining revealed extensive cytotoxicity in the BMM cultures that was minimally observed in the DC cultures (Fig. 6b). Further, the infection of DC at low MOI led to their maturation by 24 h, as indicated by the

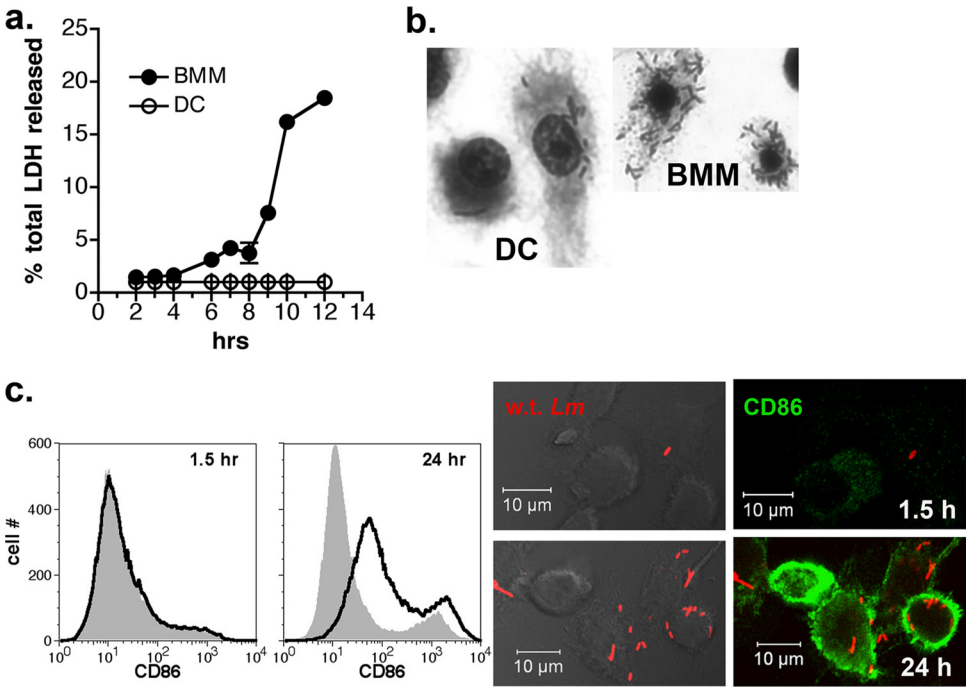

FIG. 6. Controlled growth of *L. monocytogenes* in DC preserves cellular integrity and leads to maturation at late stages of infection. (a) Cells were infected with wild-type *L. monocytogenes* per the growth experiment described for Fig. 2a, and supernatants were collected at the indicated time points for the measurement of LDH activity. Points represent the means ± standard deviations of triplicate samples, and data from one of two experiments with similar results is shown. (b) DC and BMM from the experiment depicted in panel a were fixed and stained at 24 h with Diff-Quik, illustrating cytotoxic effects and high bacterial load in BMM specifically. (c) *L. monocytogenes* infection (MOI, 0.3; 10 μg/ml gentamicin was present for the duration of the experiment) induced DC to mature by 24 h. Infected cells were harvested at 1.5 and 24 h after infection and analyzed by flow cytometry for CD86 expression. The gray-shaded histogram indicates the uninfected DC control. *L. monocytogenes* infection (red) and CD86 expression (green) also were evaluated at the same time points by immunofluorescence microscopy.

increased expression of the T-cell costimulatory molecule CD86 (Fig. 6c). Therefore, the outcome of the *L. monocytogenes* infection of DC is strikingly different from that of macrophages; although unactivated macrophages are able to support high bacterial loads and remain viable (31), unrestricted growth ultimately compromises cellular integrity. In contrast, the control of intracellular bacterial growth by DC promotes survival late in infection, a critical time period for the development of a full maturation response.

DISCUSSION

In this report, we present evidence consistent with a model in which the inefficiency of bacterial escape to the cytosol in DC compared to that in macrophages is attributed in part to differences in the early phagosomal environment encountered by *L. monocytogenes* in the two cell types. Further, our data indicate that DC limit the extent of bacterial growth in the cytosol. Therefore, DC have the capacity to inhibit the life cycle of *L. monocytogenes* both early and late in infection, and unlike macrophages they do not ultimately succumb to high bacterial loads. This finding is significant, since DC maturation during the late stages of infection is critical for the activation of an adaptive immune response.

The possibility that the enhanced trapping of *L. monocytogenes* in DC phagosomes is due to a cell type-specific inhibition of LLO function was supported by the behavior of the LLO G486D mutant in DC compared to that in BMM. The mutant had a more pronounced escape and growth defect than WT bacteria in DC, but as previously reported (13), it grew in a manner similar to that of WT bacteria in BMM. The differential phenotype of WT *L. monocytogenes* and the isogenic LLO point mutant strain in DC is consistent with an activity-related LLO defect rather than a defect resulting from the insufficient production of LLO in DC phagosomes. Further, the severity of the escape and growth phenotype of the LLO G486D mutant in DC relative to that of BMM suggests that DC phagosomes present a less permissive environment for LLO activity than BMM phagosomes.

The characterization of DC phagosomes early after infection revealed that they were positive for MHC-II, the MHC-II accessory molecule H2-DM, and LAMP2 (Fig. 3), all markers of the MHC-II-rich antigen loading vesicles (MIIC) in immature DC (12, 30). Several independent approaches demonstrated that this compartment acidified (Fig. 4 and 5). The measurement of phagosomal pH at the population level (reflecting all *L. monocytogenes*-containing phagosomes in a nonsynchronized population of infected cells) revealed that while the average pH of DC phagosomes was approaching or had reached the LLO optimum, that of BMM phagosomes had reached or surpassed it in the same time frame. The BMM acidification response reported here is consistent with that measured in individual *L. monocytogenes* phagosomes containing entrapped *L. monocytogenes*, which reached the pH opti-

mum for LLO within 5 min and began to surpass it by 30 min (5, 39). It should be emphasized that this experimental approach did not lend itself to the very early pH measurements necessary for a relevant kinetic analysis in this system; however, the results suggest that the rate or extent of phagosomal acidification in DC and BMM phagosomes is different. Although the data presented do not support phagosomal pH as a major factor in the control of *L. monocytogenes* escape to the DC cytosol, a modestly delayed acidification response nevertheless could reduce the efficiency of LLO-mediated pore formation, contributing to the DC-specific phenotype that we have reported. A similar correlation between the extent of acidification and the outcome of macrophage infection with *L. monocytogenes* has been reported. The weak base ammonium chloride inhibits (but does not completely block) phagosomal acidification, reduces LLO-mediated membrane perforation, and reduces bacterial growth (5, 28, 32).

The capacity of DC to interfere with the *L. monocytogenes* life cycle by retaining large numbers of bacteria in phagosomes that acquire markers of MIIC is significant in light of the unique antigen-processing and -presenting function of DC. MIIC of immature DC have the capacity to accumulate ingested material in a relatively intact state until maturation signals are assimilated (19, 30, 33, 44). Current studies have led to the proposal that DC limit antigen degradation by a pH-dependent mechanism that is somewhat different from that of other APC. Specifically, in this model, a balance between the activities of two macromolecular complexes, the NADPH oxidase (NOX2) and the ATP-dependent vacuolar proton pump (vATPase), which are regulated at the level of subunit assembly at the phagosomal membrane, largely controls changes in DC phagosomal pH (34). In a recent study, low and sustained levels of NOX2 activity in DC phagosomes held the pH at neutral to alkaline for a prolonged period after the ingestion of latex beads, while macrophage phagosomes acidified rapidly, reaching a pH of 5.0 within 15 min (35). Combined with low vATPase activity in immature DC phagosomes (42), this mechanism was proposed to delay the acidification, and hence the proteolytic processing, of antigens destined for cross-presentation (35). Our findings are qualitatively consistent with reported differences in phagosomal pH regulation in DC and macrophages (35). However, in our study DC phagosomes acidified within 1 h rather than remaining pH neutral. There are two possibilities to explain this difference. First, in our experimental system, immature DC received a potent maturation signal in the form of a live bacterial pathogen. Immature DC increase the assembly of vATPase subunits at the phagosomal membrane in response to inflammatory stimuli (42), which would be predicted to shift the balance between NOX2 and vATPase activities toward acidification. In addition, particle ingestion by DC proceeds by macropinocytosis as well as by phagocytosis involving multiple receptors, and this has been shown to influence the fate of ingested cargo as well as the pathway by which it is presented to T cells (10, 24, 49). As a complex cargo, *L. monocytogenes* likely is ingested by more than one route, which may differ from that of latex beads, resulting in the formation of a phagosome with different properties, including acidification potential. The relationship between the route of *L. monocytogenes* entry into DC, the fate of the bacteria (phagosomal or cytosolic), and the targeting of antigens to specific presentation pathways can be addressed in future studies using this model.

Per our previous study (50), the results of the current study suggest a DC subpopulation effect with regard to the fate of *L. monocytogenes*. Approximately 50% of infected cells contained only bacteria that colocalized with LAMP2, while 30% contained only actin$^+$ bacteria. DC derived from murine bone marrow with GM-CSF are known to be phenotypically heterogeneous (23) and most closely related functionally to inflammatory, monocyte-derived DC (48). In our studies, *L. monocytogenes* tended to be restricted by CD11c$^+$ cells that had high levels of intracellular MHC-II and H2-DM (corresponding to approximately 50% of the cells in the cultures), while CD11C$^+$ cells with intermediate to low levels tended to support bacterial escape to the cytosol (Westcott and Hiltbold, unpublished). We speculate that in this DC model, the intracellular MHC-II-high cells are developmentally more DC-like, while the population with lower levels are more monocyte-like. Such subtypes could conceivably have different endosomal properties and/or preferentially ingest *L. monocytogenes* by different routes, thus influencing the outcome of *L. monocytogenes* infection.

Although our data implicate defective LLO function in DC phagosomes, they must be considered in light of the fact that the precise mechanism by which LLO forms pores in phagosomal membranes is not clear and is known to be influenced by multiple bacterial and host-derived factors (37). Further, LLO has the ability to transiently delay phagosome/lysosome fusion in macrophages (39), as well as to transmit signals to the host cell (7, 29). Therefore, the factors that influence LLO activity in DC are likely to be complex and will require further study. Although we have demonstrated that DC phagosomes acidified within an hour to a pH that reached the LLO optimum (at least at the population level), many *L. monocytogenes* cells remained in vesicles even after several hours of infection (Fig. 2) (50). Our previous study demonstrated that vacuole-entrapped *L. monocytogenes* cells remain viable at these time points (50). One possibility to explain these observations is that in DC, bacteria are exposed for a longer period to near-neutral phagosomal pH than in macrophages, which could irreversibly inactivate LLO (38). Another possibility is that a mild acidification response delays pore formation long enough for DC phagosomes to acquire other LLO-inhibitory properties. Our data would, however, suggest a mechanism different from that of macrophages, in which phagosomal maturation to the lysosomal stage (which inhibits *L. monocytogenes* escape [18]), proceeds in conjunction with further acidification (to pH $<$ 5.0) (43). In any case, a detailed kinetic analysis of acidification at the level of individual phagosomes containing WT *L. monocytogenes* will be necessary to definitively address pH as a contributing factor in the control of *L. monocytogenes* escape to the DC cytosol.

It also is possible that other DC-specific endosomal features influence LLO function. The LLO point mutation (G486D) in the DP-L4044 strain used in the current study resides in the cholesterol-binding domain of the toxin (45), suggesting the interesting possibility that DC phagosomes present a different composition or configuration of membrane cholesterol, reducing toxin binding. Alternatively, the access of *L. monocytogenes* to the active form of GILT, a host-derived thiol reductase

involved in antigen processing (17) that recently has been shown to be required for the activation of LLO (40), may be restricted in early DC phagosomes. Finally, exposure to low-level, NOX2-generated reactive oxygen species immediately upon the arrival of *L. monocytogenes* into DC phagosomes could inactivate LLO, similarly to a scenario proposed for activated macrophages (28).

In sharp contrast to macrophages, despite the entry of roughly half of WT *L. monocytogenes* organisms into the DC cytosol (Fig. 1) (50), bacterial replication did not proceed to a significant extent past 5 h of infection, suggesting an additional level of control operating on bacteria that had left the DC phagosome (Fig. 2a) (50). Preliminary ultrastructural analysis at 7 h revealed a complex picture containing cytosolic bacteria, individual bacteria in single-membrane vesicles (suggesting they never left the initial phagosome), multiple bacteria in spacious vesicles reminiscent of those reported in macrophages from SCID mice (6), and individual bacteria in single-membrane vesicles with remnants of actin tails (Westcott and Hiltbold, unpublished). The latter suggests defective escape from secondary spreading vesicles, which requires bacterial phospholipases and LLO for the disruption of the inner and outer membranes, respectively (1). Additional studies are needed to address these findings mechanistically. However, regardless of the nature of the vesicles, the prevalence of membrane-entrapped bacteria many hours after DC infection (when bacteria are predominantly cytosolic in BMM) is consistent with the growth dynamics reported in Fig. 2 and appears to provide a significant contribution toward the maintenance of DC viability at late time points (Fig. 6).

In conclusion, we have demonstrated that the fate of *L. monocytogenes* in DC reflects the capacity of this cell type to interfere with the intracellular life cycle of the pathogen at both the phagosomal and cytosolic stages, and that this ultimately influences the fate of the host cell. The unique capacity of DC to restrict a large proportion of *L. monocytogenes* to MHC-II-rich vesicles while allowing limited bacterial replication in the cytosol may allow DC to survive the intracellular infection and receive the appropriate signals for full maturation (Fig. 6) (3, 9, 27) while at the same time promoting the efficient processing and presentation of bacterial antigens to both CD4 and CD8 T cells. *L. monocytogenes* should serve as an excellent model to address how the trafficking of a live intracellular pathogen by DC, compared to that of other APC such as macrophages, leads to the highly effective processing and presentation of antigens to the adaptive immune response.

ACKNOWLEDGMENTS

We thank Daniel Portnoy for providing bacterial strains.

This work was supported by U.S. Public Health Service grant AI057770 (E.M.H.) and WFUSM Venture Fund 20446 (M.M.W.).

REFERENCES

1. **Alberti-Segui, C., K. R. Goeden, and D. E. Higgins.** 2007. Differential function of Listeria monocytogenes listeriolysin O and phospholipases C in vacuolar dissolution following cell-to-cell spread. Cell Microbiol. **9:**179–195.
2. **Aoshi, T., B. H. Zinselmeyer, V. Konjufca, J. N. Lynch, X. Zhang, Y. Koide, and M. J. Miller.** 2008. Bacterial entry to the splenic white pulp initiates antigen presentation to $CD8^+$ T cells. Immunity **29:**476–486.
3. **Bahjat, K. S., W. Liu, E. E. Lemmens, S. P. Schoenberger, D. A. Portnoy, T. W. Dubensky, Jr., and D. G. Brockstedt.** 2006. Cytosolic entry controls $CD8^+$-T-cell potency during bacterial infection. Infect. Immun. **74:**6387–6397.
4. **Banchereau, J., and R. M. Steinman.** 1998. Dendritic cells and the control of immunity. Nature **392:**245–252.
5. **Beauregard, K. E., K. D. Lee, R. J. Collier, and J. A. Swanson.** 1997. pH-dependent perforation of macrophage phagosomes by listeriolysin O from Listeria monocytogenes. J. Exp. Med. **186:**1159–1163.
6. **Birmingham, C. L., V. Canadien, N. A. Kaniuk, B. E. Steinberg, D. E. Higgins, and J. H. Brumell.** 2008. Listeriolysin O allows Listeria monocytogenes replication in macrophage vacuoles. Nature **451:**350–354.
7. **Bou Ghanem, E. N., D. S. McElroy, and S. E. D'Orazio.** 2009. Multiple mechanisms contribute to the robust rapid gamma interferon response by $CD8^+$ T cells during Listeria monocytogenes infection. Infect. Immun. **77:**1492–1501.
8. **Bowman, E. J., A. Siebers, and K. Altendorf.** 1988. Bafilomycins: a class of inhibitors of membrane ATPases from microorganisms, animal cells, and plant cells. Proc. Natl. Acad. Sci. U. S. A. **85:**7972–7976.
9. **Brzoza, K. L., A. B. Rockel, and E. M. Hiltbold.** 2004. Cytoplasmic entry of Listeria monocytogenes enhances dendritic cell maturation and T-cell differentiation and function. J. Immunol. **173:**2641–2651.
10. **Burgdorf, S., A. Kautz, V. Bohnert, P. A. Knolle, and C. Kurts.** 2007. Distinct pathways of antigen uptake and intracellular routing in CD4 and CD8 T-cell activation. Science **316:**612–616.
11. **Cella, M., A. Engering, V. Pinet, J. Pieters, and A. Lanzavecchia.** 1997. Inflammatory stimuli induce accumulation of MHC class II complexes on dendritic cells. Nature **388:**782–787.
12. **Chow, A. Y., and I. Mellman.** 2005. Old lysosomes, new tricks: MHC II dynamics in DCs. Trends Immunol. **26:**72–78.
13. **Decatur, A. L., and D. A. Portnoy.** 2000. A PEST-like sequence in listeriolysin O essential for Listeria monocytogenes pathogenicity. Science **290:**992–995.
14. **Delamarre, L., M. Pack, H. Chang, I. Mellman, and E. S. Trombetta.** 2005. Differential lysosomal proteolysis in antigen-presenting cells determines antigen fate. Science **307:**1630–1634.
15. **Fukuda, M.** 1991. Lysosomal membrane glycoproteins. Structure, biosynthesis, and intracellular trafficking. J. Biol. Chem. **266:**21327–21330.
16. **Geoffroy, C., J. L. Gaillard, J. E. Alouf, and P. Berche.** 1987. Purification, characterization, and toxicity of the sulfhydryl-activated hemolysin listeriolysin O from Listeria monocytogenes. Infect. Immun. **55:**1641–1646.
17. **Hastings, K. T., R. L. Lackman, and P. Cresswell.** 2006. Functional requirements for the lysosomal thiol reductase GILT in MHC class II-restricted antigen processing. J. Immunol. **177:**8569–8577.
18. **Henry, R., L. Shaughnessy, M. J. Loessner, C. Alberti-Segui, D. E. Higgins, and J. A. Swanson.** 2006. Cytolysin-dependent delay of vacuole maturation in macrophages infected with Listeria monocytogenes. Cell Microbiol. **8:**107–119.
19. **Inaba, K., S. Turley, T. Iyoda, F. Yamaide, S. Shimoyama, C. Reis e Sousa, R. N. Germain, I. Mellman, and R. M. Steinman.** 2000. The formation of immunogenic major histocompatibility complex class II-peptide ligands in lysosomal compartments of dendritic cells is regulated by inflammatory stimuli. J. Exp. Med. **191:**927–936.
20. **Jones, S., and D. A. Portnoy.** 1994. Characterization of Listeria monocytogenes pathogenesis in a strain expressing perfringolysin O in place of listeriolysin O. Infect. Immun. **62:**5608–5613.
21. **Jung, S., D. Unutmaz, P. Wong, G. Sano, K. De los Santos, T. Sparwasser, S. Wu, S. Vuthoori, K. Ko, F. Zavala, E. G. Pamer, D. R. Littman, and R. A. Lang.** 2002. In vivo depletion of CD11c(+) dendritic cells abrogates priming of CD8(+) T cells by exogenous cell-associated antigens. Immunity **17:**211–220.
22. **Ladel, C. H., I. E. Flesch, J. Arnoldi, and S. H. Kaufmann.** 1994. Studies with MHC-deficient knock-out mice reveal impact of both MHC I- and MHC II-dependent T-cell responses on Listeria monocytogenes infection. J. Immunol. **153:**3116–3122.
23. **Lutz, M. B., N. Kukutsch, A. L. Ogilvie, S. Rossner, F. Koch, N. Romani, and G. Schuler.** 1999. An advanced culture method for generating large quantities of highly pure dendritic cells from mouse bone marrow. J. Immunol. Methods **223:**77–92.
24. **Lutz, M. B., P. Rovere, M. J. Kleijmeer, M. Rescigno, C. U. Assmann, V. M. Oorschot, H. J. Geuze, J. Trucy, D. Demandolx, J. Davoust, and P. Ricciardi-Castagnoli.** 1997. Intracellular routes and selective retention of antigens in mildly acidic cathepsin D/lysosome-associated membrane protein-1/MHC class II-positive vesicles in immature dendritic cells. J. Immunol. **159:**3707–3716.
25. **Macagno, A., G. Napolitani, A. Lanzavecchia, and F. Sallusto.** 2007. Duration, combination and timing: the signal integration model of dendritic cell activation. Trends Immunol. **28:**227–233.
26. **Mellman, I., and R. M. Steinman.** 2001. Dendritic cells: specialized and regulated antigen processing machines. Cell **106:**255–258.
27. **Muraille, E., R. Giannino, P. Guirnalda, I. Leiner, S. Jung, E. G. Pamer, and G. Lauvau.** 2005. Distinct in vivo dendritic cell activation by live versus killed Listeria monocytogenes. Eur. J. Immunol. **35:**1463–1471.
28. **Myers, J. T., A. W. Tsang, and J. A. Swanson.** 2003. Localized reactive oxygen and nitrogen intermediates inhibit escape of Listeria monocytogenes from vacuoles in activated macrophages. J. Immunol. **171:**5447–5453.

29. **Park, J. M., V. H. Ng, S. Maeda, R. F. Rest, and M. Karin.** 2004. Anthrolysin O and other gram-positive cytolysins are toll-like receptor 4 agonists. J. Exp. Med. **200:**1647–1655.
30. **Pierre, P., S. J. Turley, E. Gatti, M. Hull, J. Meltzer, A. Mirza, K. Inaba, R. M. Steinman, and I. Mellman.** 1997. Developmental regulation of MHC class II transport in mouse dendritic cells. Nature **388:**787–792.
31. **Portnoy, D. A., V. Auerbuch, and I. J. Glomski.** 2002. The cell biology of Listeria monocytogenes infection: the intersection of bacterial pathogenesis and cell-mediated immunity. J. Cell Biol. **158:**409–414.
32. **Portnoy, D. A., R. K. Tweten, M. Kehoe, and J. Bielecki.** 1992. Capacity of listeriolysin O, streptolysin O, and perfringolysin O to mediate growth of Bacillus subtilis within mammalian cells. Infect. Immun. **60:**2710–2717.
33. **Sallusto, F., M. Cella, C. Danieli, and A. Lanzavecchia.** 1995. Dendritic cells use macropinocytosis and the mannose receptor to concentrate macromolecules in the major histocompatibility complex class II compartment: downregulation by cytokines and bacterial products. J. Exp. Med. **182:**389–400.
34. **Savina, A., and S. Amigorena.** 2007. Phagocytosis and antigen presentation in dendritic cells. Immunol. Rev. **219:**143–156.
35. **Savina, A., C. Jancic, S. Hugues, P. Guermonprez, P. Vargas, I. C. Moura, A. M. Lennon-Dumenil, M. C. Seabra, G. Raposo, and S. Amigorena.** 2006. NOX2 controls phagosomal pH to regulate antigen processing during crosspresentation by dendritic cells. Cell **126:**205–218.
36. **Schlesinger, P. H.** 1994. Measuring the pH of pathogen-containing phagosomes. Methods Cell Biol. **45:**289–311.
37. **Schnupf, P., and D. A. Portnoy.** 2007. Listeriolysin O: a phagosome-specific lysin. Microbes Infect. **9:**1176–1187.
38. **Schuerch, D. W., E. M. Wilson-Kubalek, and R. K. Tweten.** 2005. Molecular basis of listeriolysin O pH dependence. Proc. Natl. Acad. Sci. U. S. A. **102:**12537–12542.
39. **Shaughnessy, L. M., A. D. Hoppe, K. A. Christensen, and J. A. Swanson.** 2006. Membrane perforations inhibit lysosome fusion by altering pH and calcium in Listeria monocytogenes vacuoles. Cell Microbiol. **8:**781–792.
40. **Singh, R., A. Jamieson, and P. Cresswell.** 2008. GILT is a critical host factor for Listeria monocytogenes infection. Nature **455:**1244–1247.
41. **Sun, J. C., M. A. Williams, and M. J. Bevan.** 2004. CD4+ T cells are required for the maintenance, not programming, of memory CD8+ T cells after acute infection. Nat. Immunol. **5:**927–933.
42. **Trombetta, E. S., M. Ebersold, W. Garrett, M. Pypaert, and I. Mellman.** 2003. Activation of lysosomal function during dendritic cell maturation. Science **299:**1400–1403.
43. **Trombetta, E. S., and I. Mellman.** 2005. Cell biology of antigen processing in vitro and in vivo. Annu. Rev. Immunol. **23:**975–1028.
44. **Turley, S. J., K. Inaba, W. S. Garrett, M. Ebersold, J. Unternaehrer, R. M. Steinman, and I. Mellman.** 2000. Transport of peptide-MHC class II complexes in developing dendritic cells. Science **288:**522–527.
45. **Tweten, R. K.** 2005. Cholesterol-dependent cytolysins, a family of versatile pore-forming toxins. Infect. Immun. **73:**6199–6209.
46. **Vergne, I., P. Constant, and G. Laneelle.** 1998. Phagosomal pH determination by dual fluorescence flow cytometry. Anal. Biochem. **255:**127–132.
47. **Via, L. E., R. A. Fratti, M. McFalone, E. Pagan-Ramos, D. Deretic, and V. Deretic.** 1998. Effects of cytokines on mycobacterial phagosome maturation. J. Cell Sci. **111:**897–905.
48. **Villadangos, J. A., and P. Schnorrer.** 2007. Intrinsic and cooperative antigen-presenting functions of dendritic-cell subsets in vivo. Nat. Rev. Immunol. **7:**543–555.
49. **Villadangos, J. A., P. Schnorrer, and N. S. Wilson.** 2005. Control of MHC class II antigen presentation in dendritic cells: a balance between creative and destructive forces. Immunol. Rev. **207:**191–205.
50. **Westcott, M. M., C. J. Henry, A. S. Cook, K. W. Grant, and E. M. Hiltbold.** 2007. Differential susceptibility of bone marrow-derived dendritic cells and macrophages to productive infection with Listeria monocytogenes. Cell Microbiol. **9:**1397–1411.

Editor: J. L. Flynn